Thermo-structural Induced Micromechanical Behaviour of Mo-Coated B_4C/2024 Al Alloy Nanocomposites

B. Govinda Reddy and A. Chennakesava Reddy
Department of Mechanical Engineering
Jawaharlal Nehru Technological University
Hyderabad; India
chennakesava@jntuh.ac.in

***Abstract*— 2024 aluminium alloy has excellent fatigue resistance and high strength to weight ratio. High hardness makes the application of boron carbide possible as an abrasive and cutting material. The aim of the present work was to investigate the influence of combined thermo-structural loading on the survival of B_4C/2024 metal matrix composites. For this purpose, a numerical analysis was carried out using ANSYS code. The major conclusion of the present work was that the interphase between the nanoparticles ant matrix 2024 Al alloy was ruptured at high temperature due to high thermal loading and thermal mismatch between B_4C and 2024 Al alloy.**

Keywords- 2024 Al alloy; boron carbide, thermo-structural loading; numerical analysis.

I. INTRODUCTION

Aluminium-based metal matrix composites have been widely used in many industrial applications due to their high strength-to-weight ratio [1-5]. In recent years, there has been a budding perception in using metal matrix composites for high temperature applications wherein thermal stability is major requirement such as in aircraft and automobile applications [6-10]. However, the dimensional stability depends upon the thermal mismatch between the matrix alloy and the reinforced material [11-14].

2024 aluminium alloy is an aluminium alloy, with copper as the primary alloying element. It is used in applications requiring high strength to weight ratio, as well as good fatigue resistance. Due to its high strength and fatigue resistance, 2024 is widely used in aircraft structures. A variety of chemical, physical, and mechanical properties of boron carbide ensure its wide range of applications in modern technology. High hardness (boron carbide is third in the list of the hardest compounds, the first two being diamonds and cubic boron nitride) makes the application of boron carbide possible as an abrasive and cutting material [15]. In nuclear reactors, boron carbide is used as a material for rods that controls the kinetics of nuclear fusion. Boron carbide is highly stable chemically in various aggressive environments. It is important to know the resultant influence of thermal mismatch [16] and thermal boundary resistance [17] between 2024-aluminium alloy matrix and B_4C reinforcement on the micromechanical behaviour of B_4C reinforced aluminium alloy composites. This paper describes the micromechanical behaviour subjected to both temperature and tensile loading to investigate thermal stability of B_4C/2024-aluminium alloy composites.

II. MATERIALS AND METHODS

2024-aluminium (Al) alloy and boron carbide were used, respectively, for matrix and reinforcement. ANSYS software was employed for the numerical analysis of RVE (representative volume element) models of B_4C/2024 Al alloy metal matrix nanocomposites. The boron carbide nanoparticles were coated molybdenum layer. The boron carbide nanoparticles were assumed to be spherical in the present study. The volume fraction of B_4C nanoparticles was 20%. The plane strain boundary conditions were imposed on RVE models for the numerical analysis [18-20]. The reinforcement and the matrix were discretised with plane 183 element. The interphase was discretised with contact 172 element. The operating temperatures were -150°C, -100^{0}C, -50^{0}C, 0^{0}C, 100°C. 200°C and 300°C. The RVE models were numerically tested for the yield strength of the 2024 Al alloy at different temperatures. The numerical results were validated with experimentally tested samples of the B_4C/5050 Al alloy nanocomposites.

III. RESULTS AND DISCUSSION

The average diameter of B_4C nanoparticle was 90 nm. The thickness of molybdenum layer on B_4C nanoparticles was 5 nm. Boron carbide has a complex crystal structure typical of icosahedron-based borides. There, B_{12} icosahedra form a rhombohedral lattice unit (space group: *R3m* (No. 166), lattice constants: a = 0.56 nm and c = 1.212 nm) surrounding a C-B-C chain that resides at the center of the unit cell, and both carbon atoms bridge the neighbouring three icosahedra. This structure is layered: the B_{12} icosahedra and bridging carbons form a network plane that spreads parallel to the *c*-plane and stacks along the *c*-axis. The lattice has two basic structure units – the B_{12} icosahedron and the B_6 octahedron. Because of the small size of the B_6 octahedra, they cannot interconnect. Instead, they bond to the B_{12} icosahedra in the neighbouring layer, and this decreases bonding strength in the *c*-plane [21].

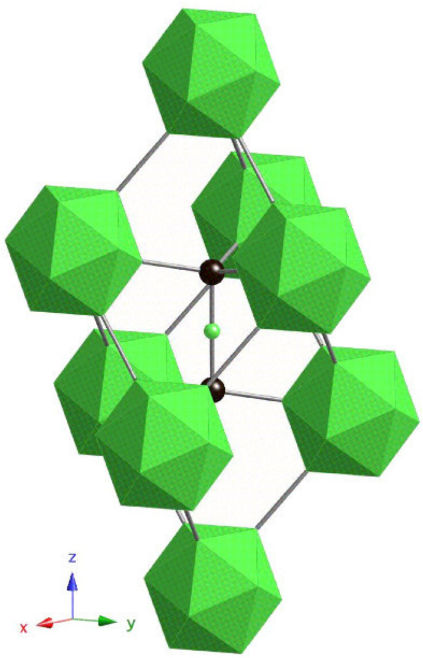

Figure 1. Unit cell of B_4C. The green sphere and icosahedra consist of boron atoms, and black spheres are carbon atoms.

The effect of temperature and structural loading on the linear dimension of RVE cell along the loading direction is shown in figure 2. It is observed that the dimension along the loading direction increases with increasing temperature of the RVE cell [14], [15]. As the temperature decreases below zero degree of temperature the dimension along the loading direction decreases because the structural loading was invariable. The same kind of trend is also observed normal to the load direction figure 3. Below zero degree of temperature thermal contraction dominates the elongation due to invariable structural loading; while above zero degree of temperature the combined effect of thermal expansion and structural elongation has been observed along the loading direction. Normal to loading direction, below zero degree of temperature the combined effect of thermal and structural contraction has been observed; while above zero degree of temperature the thermal expansion dominates the structural contraction.

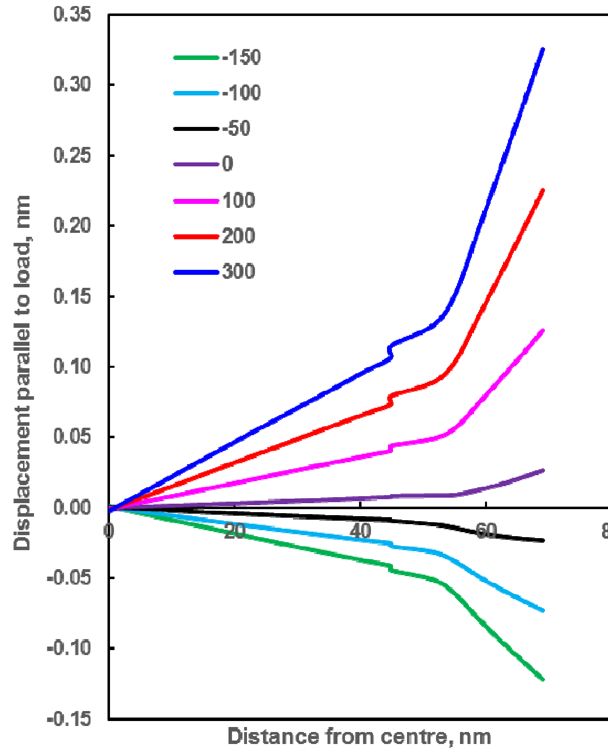

Figure 2. Effect of temperature on deformation behaviour of B_4C/2024 Al alloy nanocomposites along load direction.

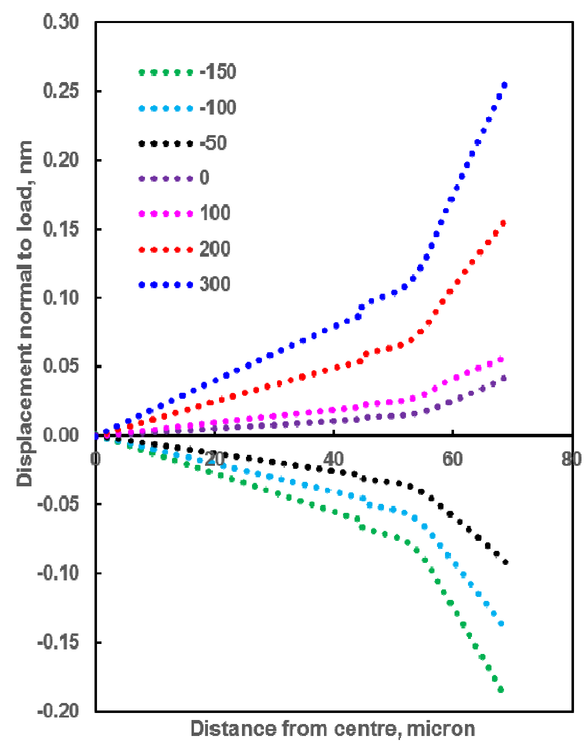

Figure 3. Effect of temperature on deformation behaviour of B_4C/2024 Al alloy nanocomposites normal to load direction.

If observed keenly the roster images as shown in figure 4, the phenomena occurred along the loading direction is reversed for the same along normal to loading direction. The influence of temperature on strains and stresses induced parallel and perpendicular to loading direction is shown in figure 5 and 6. The strain increases with an increase in the temperature in the regions of the 2024 Al alloy matrix in the directions parallel and normal to the loading. The strains are tensile in the parallel direction of tensile loading, while they are compressive in the normal direction of loading below zero degree of temperature. The strain induced in the B_4C nanoparticle is negligible either raise or fall in temperature along parallel and perpendicular directions of the applied tensile load.

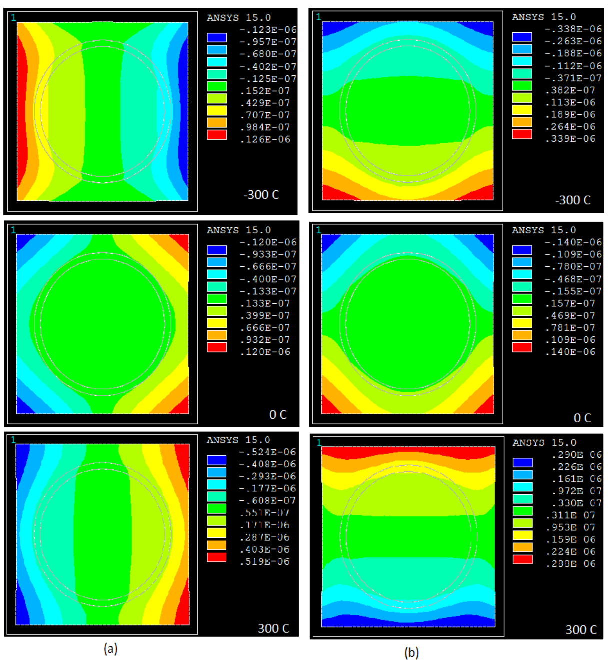

Figure 4. Effect of temperature on deformation behaviour of B_4C/2024 Al alloy nanocomposites (a) along load direction and (b) normal to load direction.

The stresses induced in the B_4C increase with increase in the temperature as shown in figure 7 and 8. It is clearly understood that the load transfer take place from the matrix to the reinforced nanoparticle via interphase. Below zero degree of temperature compressive stresses are induced in the composites in the direction normal to the loading as seen from the stress-strain diagrams (figures 9 and 10. It is observed that the interface and B_4C particles are likely to fracture at high temperatures. The same observation can be from the raster images of von Mises stresses obtain from ANSYS software code are illustrated in Fig. 13.

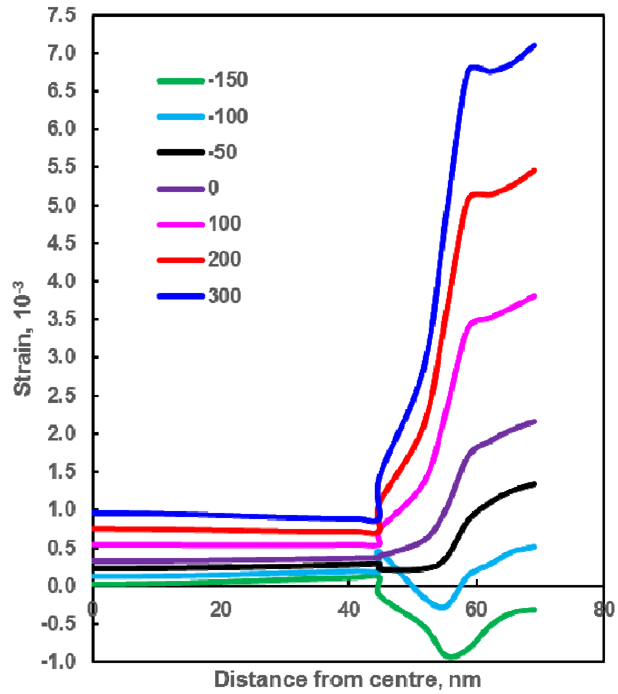

Figure 5. Effect of temperature on strains induced in B_4C/2024 Al alloy nanocomposites along load direction.

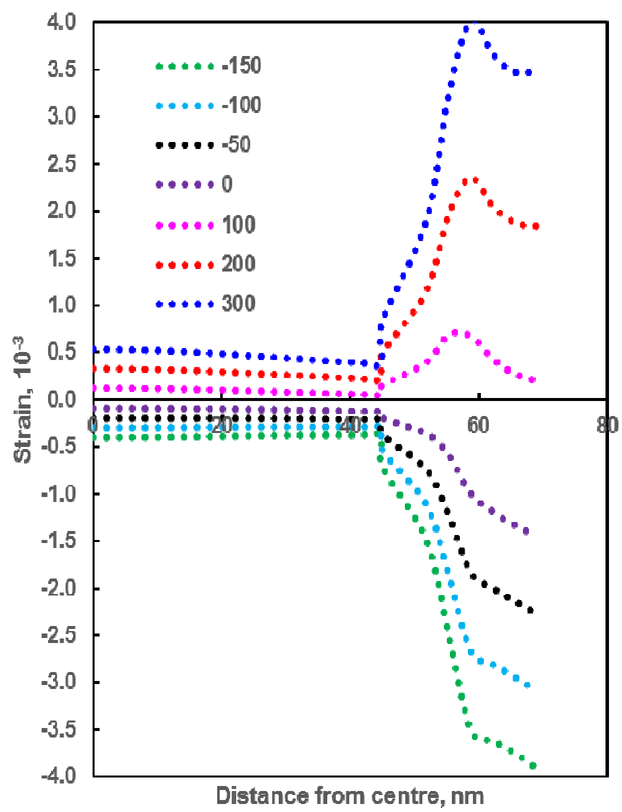

Figure 6. Effect of temperature on strains induced in B_4C/2024 Al alloy nanocomposites along normal direction to loading.

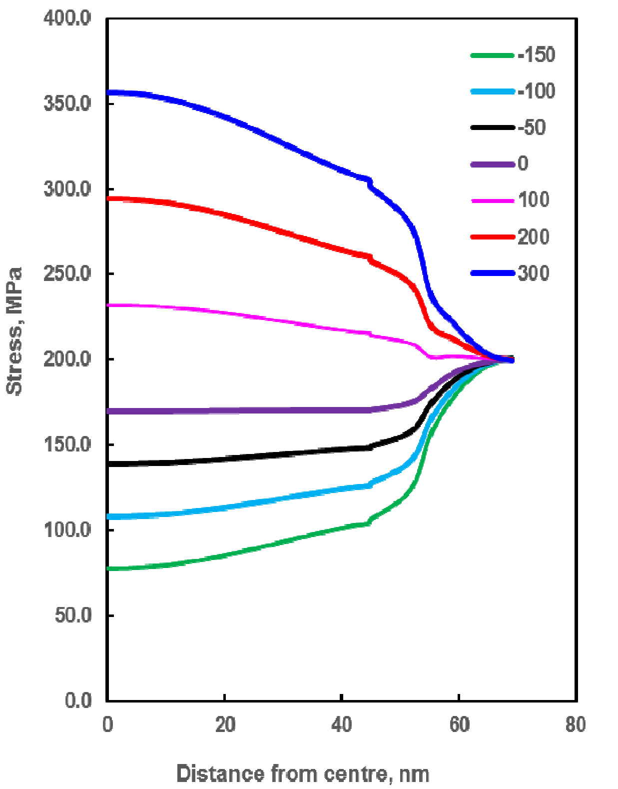

Figure 7. Effect of temperature on stresses induced in B_4C/2024 Al alloy nanocomposites along load direction.

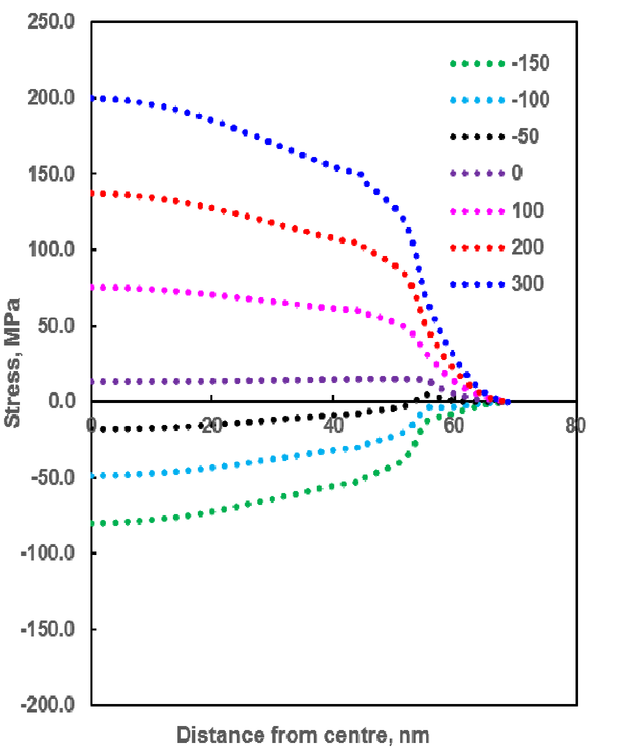

Figure 8. Effect of temperature on strains induced in B_4C/2024 Al alloy nanocomposites along normal direction to loading.

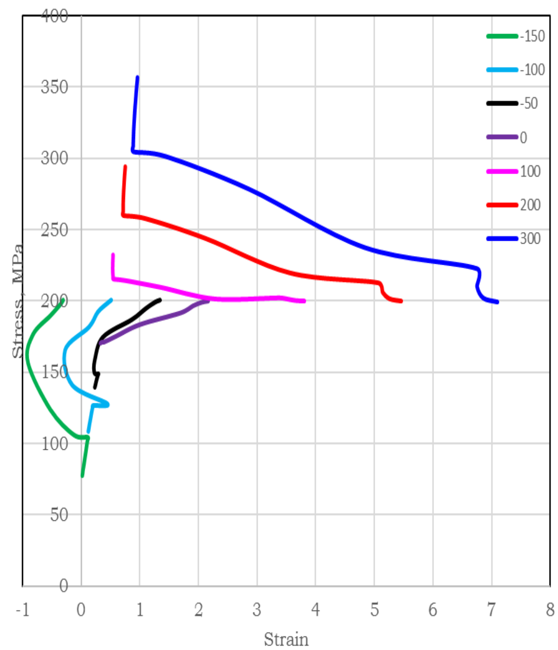

Figure 9. Stress-strain diagram of B_4C/2024 Al alloy nanocomposites along load direction.

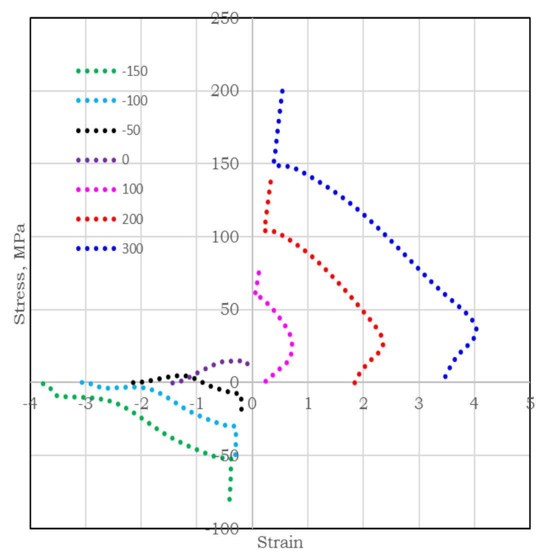

Figure 10. Stress-strain diagram of B_4C/2024 Al alloy nanocomposites along normal direction to loading.

IV. Conclusion

The thermo-strucutral induced micromechanics of B_4C/2024 Al alloy have been investigated numerically using ANSYS code. The critical conclusion of this work is that the B4C nanoparticles and intherphae are likely fracture at high temperautres along with applied stuctural loading. Under cryzonic conditions the of B_4C/2024 metal matrix composites are not subjected to heavy thermal and structural failure.

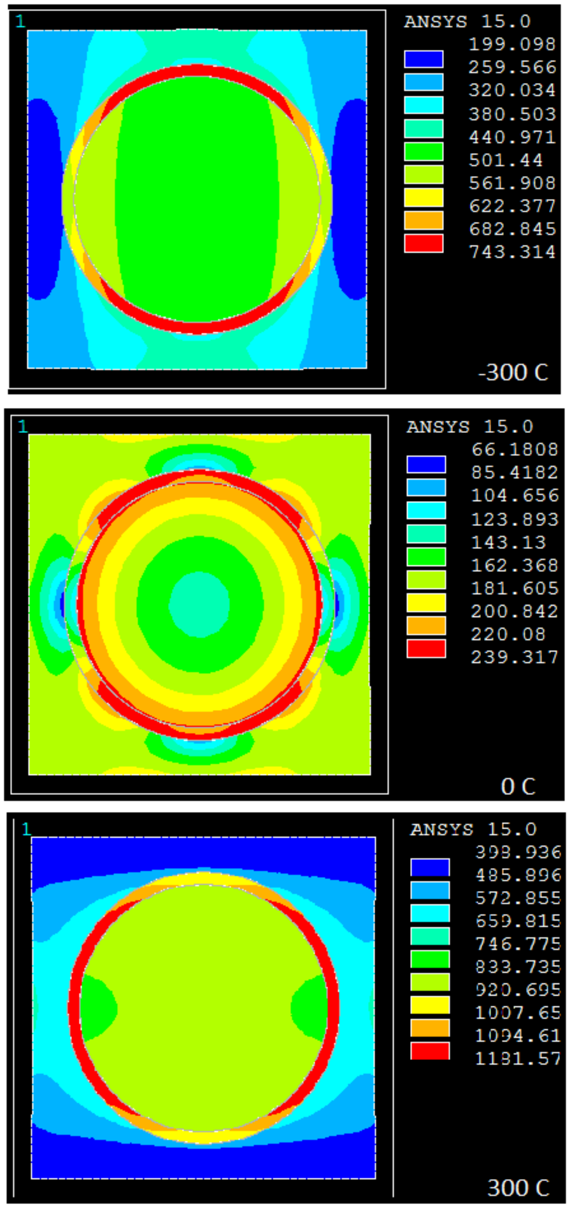

Figure 11. Raster images of von Mises stresses.

REFERENCES

1. A. C. Reddy, Essa Zitoun, Tensile properties and fracture behavior of 6061/Al2O3 metal matrix composites fabricated by low pressure die casting process, International Journal of Materials Sciences, vol.06, no.02, pp.147-157, 2011.

2. A. C. Reddy, Reckoning of Micro-stresses and interfacial Tractions in Titanium Boride/AA2024 Alloy Metal Matrix Composites, 1st International Conference on Composite Materials and Characterization, Bangalore, 14-15 March 1997, pp.195-197.

3. A. C. Reddy, B. Kotiveerachari, Influence of microstructural changes caused by ageing on wear behaviour of Al6061/SiC composites, Journal of Metallurgy & Materials Science, vol.53, no.01, pp.31-39, 2011.

4. A. C. Reddy, Influence of strain rate and temperature on superplastic behavior of sinter forged Al6061/SiC metal matrix composites, International Journal of Engineering Research & Technology, vol.04, no.02, pp.189-198, 2011.

5. A. C. Reddy, Necessity of Strain Hardening to Augment Load Bearing Capacity of AA1050/AlN Nanocomposites, International Journal of Advanced Research, vol.03, no.0 6, pp.1211-1219, 2015.

6. A. C. Reddy, Evaluation of Thermal Expansion of Al/B_4C Metal Matrix Composites, 3rd National Conference on Materials and Manufacturing Processes, Hyderabad, India, 22-25th February 2002, 196-200.

7. A. C. Reddy, Thermal Expansion Studies on Aluminum Matrix Composites with Different Reinforcement Volume Fractions of Si_3N_4 Nanoparticles, 4th International Conference on Composite Materials and Characterization, Hyderabad, India, 7-8th March 2003, pp.221-225.

8. A. C. Reddy, Sliding Wear and Micromechanical Behavior of AA1100/Titanium Oxide Metal Matrix Composites Cast by Bottom-Up Pouring, 7th International Conference on Composite Materials and Characterization, Bangalore, 11-12th December 2009, pp.205-210.

9. A. C. Reddy, Thermal Expansion Behavior of Aluminum Matrix Composites Reinforced with Fused Quartz Nanoparticles**,** National Conference on Advanced Materials and Manufacturing Techniques, Hyderabad, 08-09th March 2004, pp.350-355.

10. A. C. Reddy, Effect of TiC Nanoparticles on the Coefficient of Thermal Expansion Behavior of the Aluminum Metal Matrix Composites, 5th National Conference on Materials and Manufacturing Processes, Hyderabad, 9-10th June 2006, pp.164-168.

11. C.R. Alavala, Nano-mechanical modeling of thermoelastic behavior of AA6061/silicon oxide nanoparticulate metal matrix composites, International Journal of Science and Research, vol.05, no.01, pp.550-553, 2016.

12. C.R. Alavala, Thermoelastic Behavior of Nanoparticulate BN/AA5050 Alloy Metal Matrix Composites, International Journal of Engineering and Advanced Research Technology, vol.02, no.01, pp.6-8, 2016.

13. C.R. Alavala, Influence of Temperature on Particulate Fracture of AA2024 Alloy/Titanium Oxide nanoparticulate Metal Matrix Composites, International Journal of Scientific Engineering and Applied Science, vol.02, no.04, pp.1-6, 2016.

15. Y. D. Kovalev, S.V. Konovalihin, in Concise Encyclopedia of Self-Propagating High-Temperature Synthesis, 2017.

16. C.R. Alavala, Influence of CTE Mismatch on Debonding and Particulate Damage in AA1100 Alloy/ZrC Nanoparticulate Metal Matrix Composites, International Journal of Innovative Research in Science, Engineering and Technology, vol.05, no.03, pp.3489-3495, 2016.

17. A. C. Reddy, B. Kotiveerachari, Effect of aging condition on structure and the properties of Al-alloy / SiC composite, International Journal of Engineering and Technology, vol.02, no.06, pp.462-465, 2010.

18. C.R. Alavala, Micromechanics of Thermoelastic Behavior of AA2024/MgO Metal Matrix Composites, International Journal of Advanced Technology in Engineering and Science, vol.04, no.1, pp.33-40, 2016.

19. C.R. Alavala, Micromechanics of Thermoelastic Behavior of AA6070 Alloy/Zirconium Oxide Nanoparticle Metal Matrix Composites, International Journal of Engineering Research & Science, vol.02, no.02, pp.1-8, 2016.

20. C.R. Alavala, Effect of Thermoelastic Behavior on interfacial debonding and Particulate Fracture in AA1100/TiN Nanoparticulate Metal Matrix Composites, International Journal of Science and Research, vol.05, no.03, pp.1295-1300, 2016.

21. F.X. Zhang, F. F. Xu, T. Mori, Q. L. Liu, A. Sato, T. Tanaka. Crystal structure of new rare-earth boron-rich solids: REB28.5C4, J0rnal of Alloys and compounds, vol.329, no.01–02, pp.168–172, 2001.